The Plant Cell, Vol. 10, 1207–1216, July 1998, www.plantcell.org © 1998 American Society of Plant Physiologists

# A High-Conductance Solute Channel in the Chloroplastic Outer Envelope from Pea

**Kai Pohlmeyer,[a,1] Jürgen Soll,[a,2] Rudolf Grimm,[b] Kerstin Hill,[c,1] and Richard Wagner[c]**

[a] Botanisches Institut, Universität Kiel, D-24098 Kiel, Germany
[b] Hewlett Packard, D-76337 Waldbronn, Germany
[c] Fachbereich Biologie/Chemie, Universität Osnabrück, D-49034 Osnabrück, Germany

**The pea chloroplastic outer envelope protein OEP24 can function as a general solute channel. OEP24 is present in chloroplasts, etioplasts, and non-green root plastids. The heterologously expressed protein forms a voltage-dependent, high-conductance ($\Lambda$ = 1.3 nS in 1 M KCl), and slightly cation-selective ion channel in reconstituted proteoliposomes. The highest open probability ($P_{open} \approx 0.8$) is at 0 mV, which is consistent with the absence of a transmembrane potential across the chloroplastic outer envelope. The OEP24 channels allow the flux of triosephosphate, dicarboxylic acids, positively or negatively charged amino acids, sugars, ATP, and Pi. Structure prediction algorithms and circular dichroism spectra indicate that OEP24 contains seven amphiphilic $\beta$ strands. The primary structure of OEP24 shows no homologies to mitochondrial or bacterial porins on a primary sequence basis, and OEP24 is functionally not inhibited by cadaverine, which is a potent inhibitor of bacterial porins. We conclude that OEP24 represents a new type of solute channel in the plastidic outer envelope.**

## INTRODUCTION

Carbon dioxide reduction and its assimilation into carbohydrates, amino acids, fatty acids, and terpenoid compounds (Douce and Joyard, 1990) take place in chloroplasts. Annually, $\sim 120 \times 10^9$ tons of $CO_2$ is converted into organic substances by chloroplasts of higher land plants. In addition, chloroplasts are the sole site of nitrite and sulfate reduction (Anderson, 1990; Crawford, 1995) and their assimilation in organic compounds. Chloroplasts are surrounded by a pair of double membranes, the inner and the outer envelopes, which delimit spatially and temporally the chloroplastic compartment from the cytoplasm. Both outer and inner envelope membranes differ in structure, function, and biochemical properties but also cooperate, for example, in the synthesis of lipids or in protein translocation. The various biosynthetic functions of the chloroplasts require the existence of different and effective transport mechanisms of solutes across the envelope membranes to provide the cell with carbohydrates, organic nitrogen, and sulfur compounds. On the other hand, chloroplasts take up inorganic cations ($K^+$, $Na^+$, $Mg^{2+}$, and $Ca^{2+}$), anions (nitrite, sulfate, and phosphate), and a variety of organic biosynthetic pathway intermediates, such as phosphoenolpyruvate, dicarboxylic acids, acetate, amino acids, and ATP to fulfill their biosynthetic tasks.

The outer envelope membrane is assumed to be freely permeable for most small molecular weight solutes (Flügge and Benz, 1984), like the outer membranes of mitochondria and Gram-negative bacteria (reviewed in Benz, 1994; Nikaido, 1994). The permeability of the outer membranes of mitochondria and Gram-negative bacteria is caused by pore-forming proteins, designated porins, which share structural and functional features. Similar to these systems, the osmotic barrier against the cytosol is formed by the inner envelope membrane, containing specific carrier proteins of which some have been identified at the functional (reviewed in Flügge and Heldt, 1991) and the molecular (Weber et al., 1995; Fischer et al., 1997; Neuhaus et al., 1997) level.

Recently, we have identified a channel-forming protein, OEP16, in the outer envelope membrane of pea chloroplasts. OEP16 selectively passes amino acids but excludes sugars, sugar phosphates, and organic acids (Pohlmeyer et al., 1997). Furthermore, a number of electrophysiological studies using either giant chloroplasts of Nitellopsis (Pottosin, 1992, 1993) or isolated envelope membrane vesicles from spinach (Flügge and Benz, 1984; Heiber et al., 1995) have described the presence of different voltage-dependent, high-conductance channels in the envelope membranes. None of these chloroplast channels has been identified, and thus, our understanding of how solutes cross the chloroplastic outer envelope is extremely limited.

Here, we present a molecular characterization and functional reconstitution of a 24-kD chloroplastic outer envelope membrane protein, OEP24. The primary structure of OEP24

[1] These authors contributed equally to this work.
[2] To whom correspondence should be addressed at Botanisches Institut, Universität Kiel, Am Botanischen Garten 1-9, D-24118 Kiel, Germany. E-mail jsoll@bot.uni-kiel.de; fax 49-431-880-4222.

shows no homology to classic porins but shares structural and functional features. OEP24 reconstituted into liposomes forms a voltage-dependent, slightly cation-selective, high-conductance channel, which could conduct a variety of substrates, for example, sugars, sugar phosphates, dicarboxylic acids, amino acids, Pi, and ATP, across the membrane.

## RESULTS

With the exception of OEP16 (Pohlmeyer et al., 1997), no solute channels have been identified in the chloroplastic outer envelope. Accordingly, we have started to identify pore-forming proteins by using the following rationale. Solute transport, including protein transport, is a major task of the outer envelope membrane. Thus, proteins involved in transport should be prominent in this membrane, as has been shown for subunits of the protein translocon of chloroplastic outer envelopes Toc86, Toc75, and Toc34 (reviewed in Lübeck et al., 1997; Heins et al., 1998) or the amino acid–selective channel protein OEP16. An additional criterion that is common to many channel proteins is their resistance to proteolysis. One of the chloroplastic outer envelope proteins that met this criterion was prominent after SDS-PAGE and had an apparent molecular mass of 24 kD (data not shown). Therefore, N-terminal and internal protein sequences were obtained for the pea chloroplastic 24-kD protein, and a cDNA clone was isolated. Both peptide sequences were found in the deduced open reading frame, thus demonstrating that the cDNA clone peacOEP24 codes for the 24-kD protein (Figure 1A). The deduced amino acid sequence of peacOEP24 starts with the N-terminal protein sequence, indicating that OEP24 contains no cleavable chloroplast targeting signal. The calculated molecular mass of the deduced protein is 23.4 kD, and the protein has a pI of 9.1. The high content of hydrophilic amino acids (49%) is unusual for an integral membrane protein. A database search revealed no significant homologies to other proteins, except to expressed sequence tags from rice (EMBL accession numbers D41099 and D40417) and oilseed rape (EMBL accession number L30117), indicating that the 24-kD protein is present in both monocotyledonous and dicotyledonous plants.

An antiserum was raised against the recombinant protein in a rabbit and used to study the subcellular and organ-specific distribution of the endogenous 24-kD protein. As shown in Figure 1B (lane 1), the antiserum predominantly recognized a polypeptide in the purified outer envelopes from pea chloroplasts. Minor cross-reactivity was observed with purified inner envelope vesicles (Figure 1B, lane 2), which is consistent with the reported cross-contamination of inner envelope membranes with outer envelope membranes (Keegstra and Youssif, 1986). The antiserum cross-reacted with neither stromal nor thylakoid proteins (Figure 1B, lanes 3 and 4) nor with a total membrane fraction from potato mitochondria (Figure 1B, lane 5). These data establish that the cDNA clone peacOEP24 codes for a chloroplastic outer envelope protein, which we named OEP24. OEP24 is present in plastids of roots, shoots, and leaves of pea plants grown either in the dark or in the light, demonstrating its presence in different plastid types (Figure 1C).

After treatment of purified chloroplastic outer envelope vesicles with 0.1 M $Na_2CO_3$, pH 11.5, or 1 M NaCl, OEP24 was recovered in the insoluble membrane fraction (Figure 2A), indicating that it is an integral membrane protein (Fujiki et al., 1982). Hydropathy analysis of the deduced amino acid sequence and secondary structure prediction algorithms did not reveal any amino acid stretches sufficient to span the membrane in a helical conformation. However, seven putative amphiphilic β strands were predicted (Figure 2B), indicative of a pore-forming protein. To confirm the secondary structure prediction, circular dichroism (CD) spectra were obtained from heterologously expressed OEP24. The protein was recovered from insoluble inclusion bodies (Figure

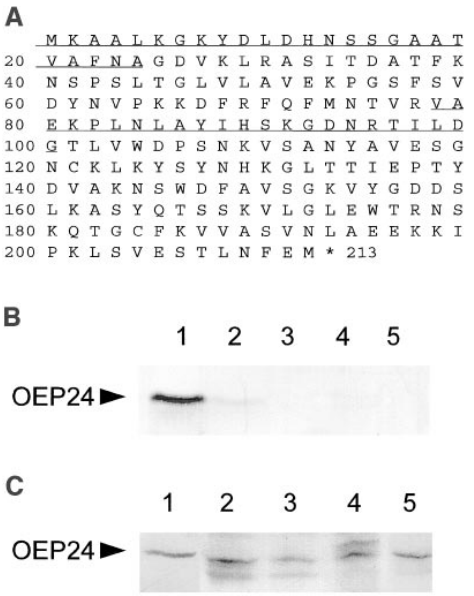


**Figure 1.** OEP24 Is Localized in the Chloroplastic Outer Envelope from Pea and Present in Different Plastid Types.

**(A)** The amino acid sequence of OEP24 as deduced from the cDNA clone peacOEP24 (EMBL accession number AJ001009). Amino acids verified by peptide sequencing are underlined. The asterisk indicates the end of the protein sequence.

**(B)** Immunoblot analysis of the subcellular localization of OEP24. Lane 1, outer envelope; lane 2, inner envelope; lane 3, thylakoids; lane 4, stroma; and lane 5, total mitochondrial membranes from potato equivalent to 20 μg of protein.

**(C)** Expression of OEP24 in different pea plant organs. Lane 1, 5 μg of pea chloroplastic outer envelope protein; and lanes 2 to 5, total membrane protein (100 μg per lane) from green leaves (lane 2), green shoots (lane 3), roots (lane 4), and etiolated leaves (lane 5), respectively.

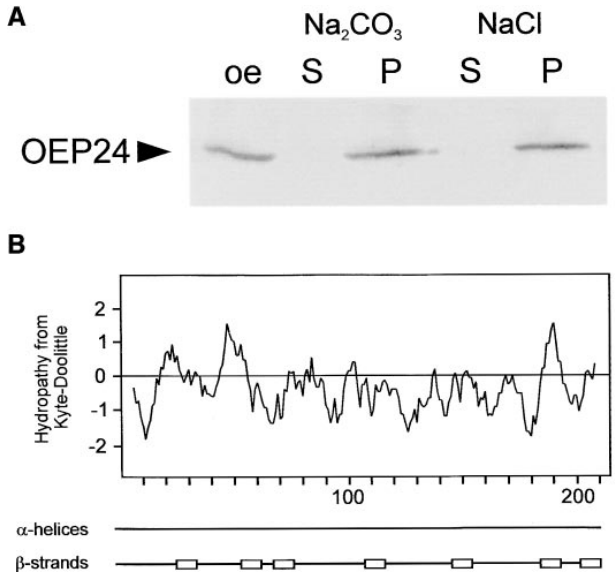


**Figure 2.** OEP24 Behaves as an Integral Membrane Protein.

**(A)** Pea chloroplastic outer envelopes (oe, 10 μg of protein) were either treated or not treated with 0.1 M $Na_2CO_3$, pH 11.5, or 1 M NaCl and separated into a soluble (S) and insoluble (P) protein fraction by centrifugation. The results of the immunoblot analysis are shown.

**(B)** Shown is a hydropathy analysis of the deduced amino acid sequence of OEP24 (Kyte and Doolittle, 1982) and secondary structure prediction by the algorithm of Claros and von Heijne (1994). The x-axis indicates number of amino acids; the y-axis is the hydropathy index (without dimension). The open rectangles indicate the positions of the β-strands.

3C, lane 1) and purified after denaturation in 6 M urea by successive anion and cation exchange chromatography, respectively (Figures 3A and 3B). This procedure resulted in an OEP24 preparation that was purified to apparent homogeneity (Figure 3C, lane 3).

Purified OEP24 was reconstituted into liposomes (OEP24 liposomes), and the CD spectra were measured to determine changes in the relative abundance of secondary structure motifs during reconstitution (Figure 4A). Fractions of secondary structure calculated by the self-consistent method of Sreerama and Woody (1994) showed that the β sheet content increased drastically after reconstitution of the purified protein into liposomes (Figures 4A and 4B), whereas the spectra of urea-denatured OEP24 showed that the protein adopts a largely extended conformation. In the liposome membrane, the fraction of β sheets comprises ~50% of the OEP24 secondary structure motifs (Figure 4B). These calculated values corroborate well with the secondary structure prediction, which also indicates that β sheets are the most frequently occurring secondary structure in the folded protein.

To examine whether OEP24 forms a pore in vitro, we used the OEP24 liposomes for electrophysiological measurements with the bilayer technique. After fusion of OEP24 liposomes with the bilayer, single-channel currents could be observed (Figure 5A). At low membrane potentials, the channels were mainly open, and they were closed when higher membrane potentials were applied (Figure 5A). Figure 5 shows current recordings from a bilayer containing three active channels after application of a voltage step from 0 to +160 mV at $t = 0$. At higher membrane potentials, the same channel behavior was observed when voltage ramps were applied (Figure 5B). To estimate the ion selectivity and relative permeabilities of the OEP24 channel, the reversal potential $V_{rev}$ was determined under a variety of ionic conditions (Table 1). The relative permeabilities to $Ca^{2+}$:$K^+$:$Cl^-$ ≅ 3.0:1:0.27 were calculated according to Allen and Sanders (1995). This shows that the OEP24 channel is highly permeable for $Ca^{2+}$ ions and has a slight preference for cations (Table 1). Additional measurements of the relative permeability of the OEP24 channel yielded the following information: $Cs^+(1.2) > K^+(1) > Na^+(0.7) > Li^+(0.6) > Tris^+(0.3) > TEA^+(0.1)$ (Table

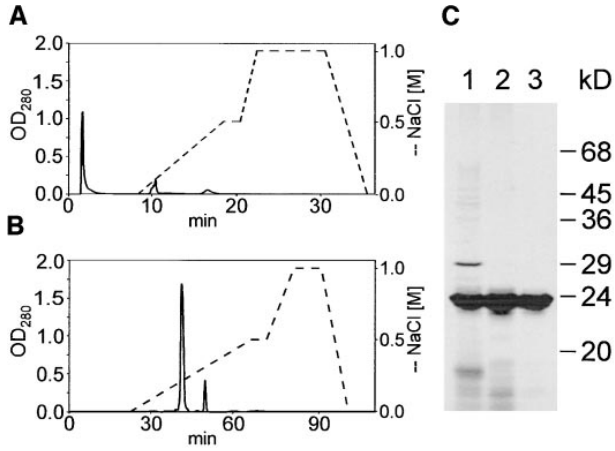


**Figure 3.** Expression and Purification of OEP24.

OEP24 was expressed in *E. coli* BL21(DE3) and recovered from insoluble inclusion bodies.

**(A)** Insoluble protein was solubilized in 6 M urea and applied to an anion exchange chromatography matrix in 25 mM Hepes-KOH, pH 7.6, 6 M urea, 1 mM EDTA, and 1 mM β-mercaptoethanol. The column was developed with gradients from 0 to 0.5 and 0.5 to 1 M NaCl under the conditions mentioned above.

**(B)** OEP24, which was recovered in the flowthrough, was further purified by cation exchange chromatography. Proteins were eluted by linear gradients from 0 to 0.5 and 0.5 to 1 M NaCl. OEP24 eluted at ~100 mM NaCl.

**(C)** Lane 1, protein pattern of OEP24 recovered from inclusion bodies; lane 2, OEP24 obtained from the anion exchange flowthrough; and lane 3, OEP24 obtained by cation exchange chromatography from the 100 mM NaCl eluant. A silver-stained SDS–polyacrylamide gel is shown. Numbers at right indicate molecular mass markers in kilodaltons.

In **(A)** and **(B)**, dotted lines indicate the salt gradient.

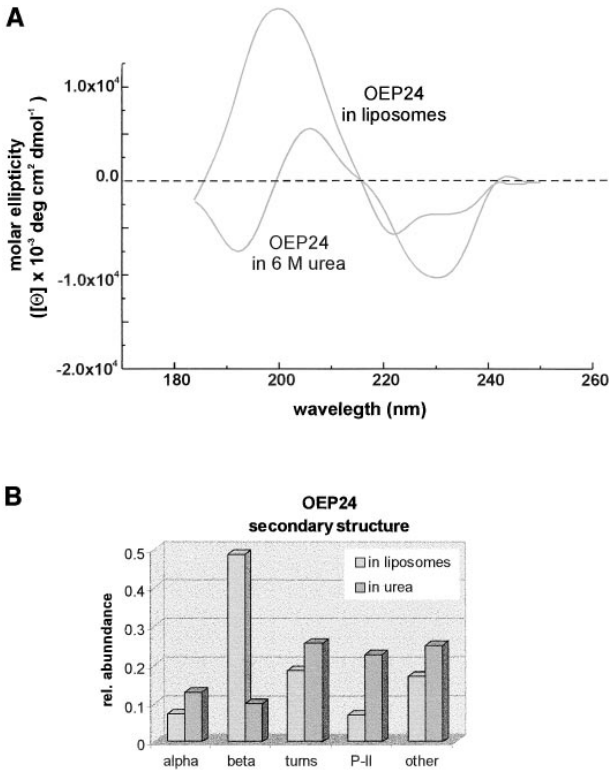


**Figure 4.** Structural Analysis of OEP24.

**(A)** CD spectra of OEP24 either denatured in 6 M urea or reconstituted into liposomes. CD spectra were recorded between 180 and 250 nm on a Jasco 720 CD spectropolarimeter, as described in Methods. Dotted line at center indicates the zero line. deg, degree.
**(B)** Relative (rel.) abundance of OEP24 secondary structure either denatured in 6 M urea or reconstituted into liposomes, according to Sreerama and Woody (1994). P-II, disturbed helix in the presence of two prolines.

1, where TEA is tetraethylamine and the numbers in parentheses are relative permeability). This series roughly reflects the relative mobility of the corresponding ions in solution. Therefore, these ions are likely to be transferred across the membrane without changes in their hydration status, indicating that the channel forms a wide pore and that its interaction with these ions is weak (Hille, 1992). The slope conductance as calculated from Figure 5A is $\Lambda = 250 \pm 15$ pS (250/20 mM KCl, *cis*/*trans*). From the current voltage relationship of the open single channel, we obtained a similar slope conductance of $\Lambda = 250 \pm 12$ pS. In bilayer experiments with symmetrical 1 molal KCl buffer, we calculated a slope conductance of $\Lambda = 2.1$ nS for the OEP24 channel (Figure 6C).

During the course of the experiments, we also tested the electrophysiological properties of the reconstituted OEP24 protein that had been recovered as insoluble inclusion bodies without further purification (see Methods). As observed for OEP24 purified by successive ion exchange chromatography, channels closed immediately when higher membrane potentials were applied (Figure 6A). The other electrophysiological channel properties, that is, selectivity, voltage dependence, and conductance, as well as the CD spectra of the reconstituted protein (data not shown) obtained by using the one-step preparation protocol and those of OEP24 obtained by the more elaborate purification protocol, were identical. Therefore, in the experiments described below, we used OEP24 recovered from inclusion bodies.

The voltage dependence of the channel open probability is shown in Figure 6B. From this result (Figure 6B), it is apparent that the highest open probability ($P_{open}$) was maximal at a membrane potential of $V_m = 0$ mV, decreasing with increasing positive or negative potentials. These measurements were performed under conditions in which channel gating at a given voltage is expected to occur at equilibrium. Voltages were applied for 5 min to approach equilibrium, and only the current recordings of the last minute were used to calculate $P_{open}$. Above $V_m = \pm 150$ mV, the OEP24 channel is closed completely. In symmetrical buffers, the OEP24 channel showed a linear current–voltage relationship (Figure 5C), whereas the concentration dependence of the channel conductance approached saturation behavior at very high nonphysiological KCl concentrations (Figure 6C). Assuming Michaelis-Menten–type saturating ion fluxes, the limiting conductance of the channel would be $\Lambda_{max}$ at $\approx$ 6.2 nS. However, at physiological solute concentrations, the solute fluxes through the OEP24 pore would be almost linear. By the assumption of a simple, water-filled pore, a diameter of $\sim$3 nm can be calculated from the conductivities (Hille, 1992). The permeability of charged solutes was examined by studying changes in the reversal potential ($E_{rev}$) resulting from the addition of the solutes to either the *cis* or *trans*-compartments (see Table 1).

To assess the permeability of OEP24 for different noncharged and charged solutes, we used the osmotically induced fusion of OEP24 liposomes with the planar bilayer. By using this technique, we could determine whether fusion of bilayer-attached liposomes was completely due to their osmotically induced swelling achieved by the addition of the osmoticum to the *cis*-compartment of the bilayer. By using membrane impermeable solutes, the presence of an open channel permeable for the osmotically active solute is essential (Miller et al., 1976; Woodbury and Miller, 1990; for details, see Methods). Because the OEP24 channel has its highest open probability at $V_m = 0$ mV, this method is suited ideally for testing permeation of substances through the open pore. As shown in Table 2, all of the examined substrates, which are of physiological relevance to chloroplast metabolism, were able to pass through the OEP24 channel. In the presence of sucrose, fusion events were detectable at only $\leqslant$1% of the attempts, indicating that permeation through OEP24 channels is very slow or impossible (see below). TEA and Hepes also cannot permeate into the proteoliposomes. The main products of photosynthesis, such as

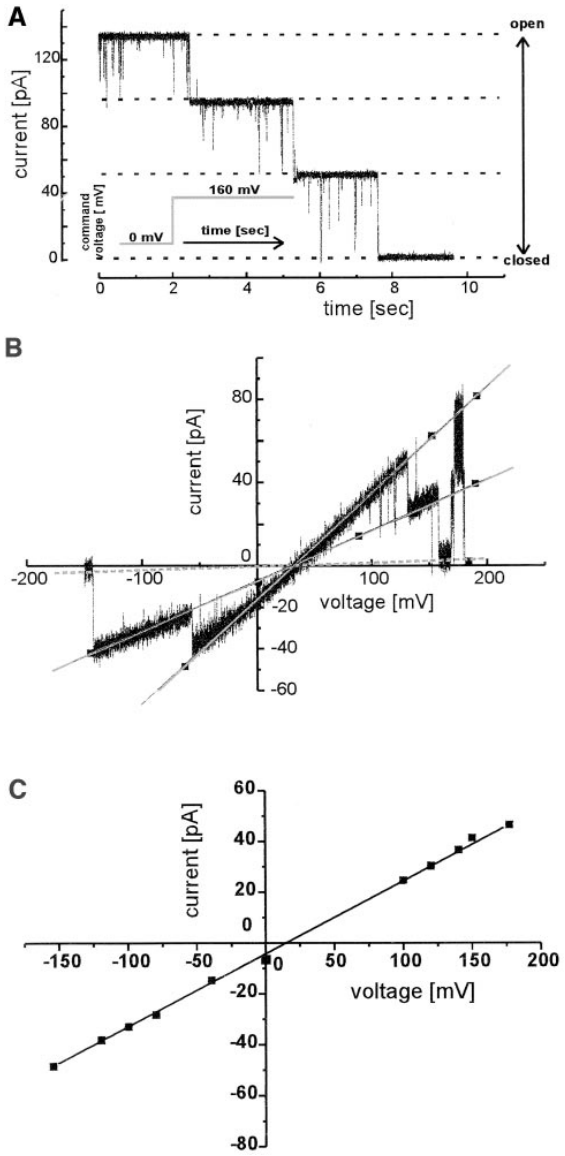


**Figure 5.** Electrophysiological Properties of Purified Recombinant OEP24.

**(A)** Current trace from a bilayer containing three active channel copies in response to a voltage jump from 0 to 160 mV at $t = 0$. The *cis*-chamber contained 250 mM KCl and 10 mM $CaCl_2$, and the *trans*-compartment contained 20 mM KCl. The dotted line indicates the difference in current upon closure of one channel.

**(B)** Current–voltage relationship of OEP24 after a voltage sweep ($\Delta = 20$ mV/sec) from $-150$ mV to $+180$ mV. Solutions are as given in **(A)**. The bilayer contained two active pores, which closed at high positive and negative potentials.

**(C)** Current–voltage relationship of single-channel conductance ($n \geq 3$ for each data point). Experimental conditions are as given in **(A)**. The line represents the linear regression of the data with a slope conductance of $\Lambda = 291 \pm 4.4$ pS.

hexosephosphates, triosephosphates, and ATP, which are exported to the cytosol, are channeled with the same efficiency as acetate, $\alpha$-ketoglutarate, or Pi, which are taken up by mature chloroplasts (Preiss et al., 1993). All of the tested amino acids could penetrate into the liposomes through the OEP24 channel. Cadaverine, an effective inhibitor of bacterial porins, is also channeled by OEP24.

The light-scattering properties of OEP24 liposomes also were used to investigate the permeability of OEP24 to different noncharged or charged solutes. Turbidity changes of liposome suspension are related mainly to volume changes. After a fast increase in the osmolarity of the surrounding medium, the following is to be expected. If the liposome membrane is impermeable to the osmoticum, the liposomes will shrink. Little or no volume change is expected when the membrane is permeable to the solute. Depending on liposome status (unilamellar or multilamellar) and variation in the size distribution of vesicles and their average size (Yoshikawa et al., 1983; Viera et al., 1996), shrinking of the liposomes may induce positive or negative changes of turbidity. The size distribution can be measured qualitatively by the wavelength dependence of the turbidity, which can be approximated to $\lambda^{-(x)}$ in the region from 350 to 800 nm, where $-(x)$ is a variable fit parameter. The wider the size distribution becomes, the smaller is the value of the exponent (x) (Yoshikawa et al., 1983). Changes in the osmolarity from $\Delta$10 mOsm to $\Delta$100 mOsm (where Osm stands for osmolar) by the addition of KCl and sucrose to liposomes containing no proteins induced turbidity changes in the same direction ($[\Delta A/A]_{400\ nm} = -0.08$). For some solutes, only less concentrated stock solutions could be prepared, for example, ATP (Table 2). The lower $\Delta$Osm values yielded smaller turbidity changes with the same sign ($[\Delta A/A]_{400\ nm} \leq -0.08$).

For OEP24 liposomes, the addition of KCl, sucrose, and dextran (apparent molecular mass of 10 kD) produced different changes in suspension turbidity. Although the $(\Delta Osm)_{KCl}$ of 100 mOsm produced a fast turbidity change of $(\Delta A/A)_{400\ nm} \leq 0.08$, the addition of sucrose ($[\Delta Osm]_{sucrose}$ of 100 mOsm) produced a slowly increasing turbidity change

**Table 1.** Relative Ion Permeability of OEP24 Liposomes

| *cis* | *trans* | $E_{rev}$ ($\pm$ SD) |
|---|---|---|
| 250 mM KCl | 250 mM KCl | |
| 5 mM $CaCl_2$ | 5 mM $CaCl_2$ | 0 $\pm$ 0.5 mV ($n = 4$) |
| 250 mM KCl | 25 mM KCl | |
| 5 mM $CaCl_2$ | 5 mM $CaCl_2$ | 26 $\pm$ 2.5 mV ($n = 4$) |
| 250 mM KCl | 250 mM KCl | |
| 5 mM $CaCl_2$ | 25 mM $CaCl_2$ | 12 $\pm$ 1.8 mV ($n = 4$) |
| 250 mM KCl | 250 mM $CaCl_2$ | $-5$ $\pm$ 0.5 mV ($n = 4$) |
| 250 mM KCl | 250 mM LiCl | 14 $\pm$ 1.3 mV ($n = 4$) |
| 250 mM KCl | 250 mM $CaCl_2$ | 9 $\pm$ 0.8 mV ($n = 4$) |
| 250 mM TEA-Cl | 250 mM KCl | $-32$ $\pm$ 1.2 mV ($n = 3$) |
| 250 mM Tris-Cl | 250 mM KCl | $-30$ $\pm$ 2.2 mV ($n = 3$) |

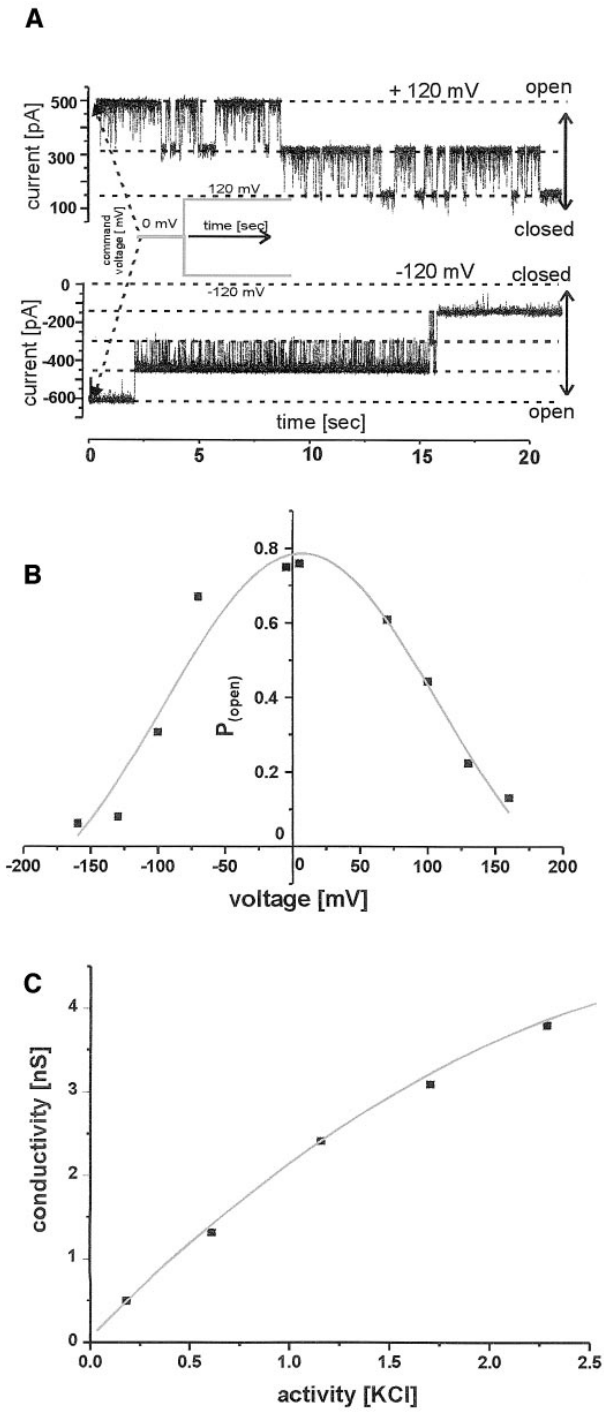


**Figure 6.** Electrophysiological Properties of Reconstituted OEP24 Obtained from Insoluble Inclusion Bodies.

**(A)** Current traces after voltage jumps from 0 to +120 mV and from 0 to −120 mV. *cis*- and *trans*-compartments contained symmetrical 250 mM KCl.

**(B)** Open probabilities of the OEP24 pore. Conditions are as given in **(A)**. To approach the equilibrium, given voltages were applied for 5 min, but only the mean current of the last minute was used as a representative steady state current.

**(C)** Single-channel conductance at increasing KCl activity of the solution, revealing the saturation behavior of OEP24. Each data point represents the average of three independent measurements.

approaching a value of $(\Delta A/A)_{400\ nm} = 0.07$, with a half-time of ~1.5 min. When dextran (apparent molecular mass of 10 kD) of $(\Delta Osm)_{dextran} = 25$ mOsm was added to the OEP24 liposome suspension, a turbidity change of $(\Delta A/A)_{400\ nm} = -0.018$, which is a value almost identical to the one obtained for control liposomes ($[\Delta A/A]_{400\ nm} = -0.016$), was observed, indicating that dextran cannot permeate the OEP24 channel. Concomitantly, no fusion of the OEP24 liposomes to planar bilayers was observed with dextran (apparent molecular mass of 10 kD) as the osmotically active solute. Although turbidity measurements have to be interpreted with caution, they can be interpreted as follows when combined with the results of bilayer fusion and the electrical measurements. (1) OEP24 is impermeable to dextran (apparent molecular mass of 10 kD). With this compound as the osmotically active solute, no fusion of OEP24 liposomes to planar bilayers was observed, and $(\Delta Osm)_{sucrose} = 25$ mOsm produced a moderate shrinkage of the liposomes. (2) OEP24 is only slowly permeable to sucrose. With sucrose as the osmotically active solute, fusion of OEP24 liposomes to planar bilayers was observed only very rarely. (With the applied fusion technique, the transit time of liposomes passing the bilayer area and allowing fusion to occur is <30 sec.) (3) OEP24 is highly permeable to KCl. Ion currents through the OEP24 pore carried by $K^+$ and $Cl^-$ have been measured (see above). With KCl as an osmotically active solute, easy fusion of the OEP24 liposomes to planar bilayers was observed, and $(\Delta Osm)_{KCl} = 100$ mOsm produced a fast increase in the liposome volume.

Based on these data, we used the turbidity measurements to reinvestigate qualitatively the permeability of OEP24 to different noncharged solutes, as listed in Table 2. The results obtained for the permeability of OEP24 to different solutes by measuring changes in turbidity gave identical results in comparison with the electrical measurements to the osmotical-induced fusion of OEP24 liposomes. Taken together, these results show that the OEP24 forms a large rather nonselective pore.

## DISCUSSION

The different types of plastids are important cellular compartments involved in both the synthesis and storage of various compounds, for example, carbohydrates, lipids, and amino acids. Whereas the inner envelope membrane contains a number of already identified carrier proteins (Weber

**Table 2.** Selectivity of Reconstituted OEP24 Channels

| Substrate | Permeability[a] |
|---|---|
| Glycine | + |
| Valine | + |
| Arginine | + |
| Glutamate | + |
| Aspartate | (+)[b] |
| Cadaverine | +[b] |
| Manitol | +[b] |
| Sucrose | (+)[b] |
| Glucose | +[b] |
| Glucose 6-phosphate | + |
| Gluconate | +[b] |
| Phosphoglyceric acid | + |
| Dihydroxyacetone | + |
| α-Ketoglutarate | + |
| Malate | + |
| Acetate | + |
| ATP | +[b] |
| Tris(hydroxymethyl) aminomethane | +[b] |
| Tetraethylamine | (+)[b] |
| Hepes | (+)[b] |

[a] +, highly permeable; (+), slowly permeable.
[b] Identical results obtained by changes in turbidity measurements of OEP24 liposomes. Solutes not marked were not tested.

et al., 1995; Fischer et al., 1997; Neuhaus et al., 1997), only two channel proteins of the outer envelope, namely, Toc75 and OEP16, have been described. Toc75 forms the protein translocation channel of the outer envelope protein translocon (Hinnah et al., 1997). OEP16 is an amino-selective channel protein (Pohlmeyer et al., 1997) but not a general solute channel protein. In vitro electrophysiological measurements using heterologously expressed and reconstituted protein show that OEP24 forms a voltage-dependent, high-conductance solute channel with a slight selectivity for cations. Together, these results strongly suggest that OEP24 also forms a general solute channel in situ.

From the protein-to-lipid ratio during reconstitution, we calculate that a maximum (100% reconstitution efficiency) of 15 OEP24 molecules per lipid vesicle can be obtained after reconstitution (Hinnah et al., 1997). Purified OEP24 does not contain >1% contamination by other proteins, as was determined from the silver-stained SDS–polyacrylamide gel. Thus, we expect (100% reconstitution; apparent molecular mass contamination of 30 kD) 0.1 molecules per lipid vesicle of a potential contaminant channel protein. In the course of the experiments, we observed that fusion events of single liposomes always led to multiple incorporation of active channels. Coincident fusion of at least 10 vesicles containing an average of 0.1 channel molecules within a time window of ~1 msec would be required to produce the observed simultaneous appearance of channel activity, which is extremely unlikely. Recently, the electrophysiological characterization of Toc75 (Hinnah et al., 1997) and OEP16 (Pohlmeyer et al., 1997) was reported. Both reports revealed properties very different from those of OEP24, even though the same expression system and *Escherichia coli* strains were used in all cases. Furthermore, cadaverine, an effective inhibitor of *E. coli* porins (DeLa Vega and Delcour, 1996), permeates through the OEP24 channel. Therefore, it seems most unlikely that the channel activity measured in our OEP24 preparations is due to a protein contamination from *E. coli.*

OEP24 shows no homologies in its primary structure to other channel or porinlike proteins. However, secondary structure prediction algorithms and CD spectra of OEP24 liposomes indicate the presence of amphipathic β strands, which is the typical secondary structure of bacterial and mitochondrial porins (Cowan et al., 1992; De Pinto et al., 1991). The high content of hydrophilic amino acids in the primary sequence also seems to be a common feature of pore-forming proteins (Benz, 1994; Nikaido, 1994; Hinnah et al., 1997; Pohlmeyer et al., 1997). The high conductivity of OEP24 channels (2.1 nS in 1 molal KCl) and the calculated diameter of the aqueous pore of 2.5 to 3 nm indicate that the channel is formed by an oligomer. Chemical cross-linking of isolated purified outer envelope membranes indicates that OEP24 can form a homodimer, whereas heterooligomeric complexes were not observed (K. Pohlmeyer and J. Soll, unpublished results).

OEP24 is present in differently developed plastids, that is, chloroplasts, etioplasts, and non-green plastids from roots. Recently, a 30-kD protein was described from pea proplastids that showed significant homology to mitochondrial porins from potato (Fischer et al., 1994; Heins et al., 1994). Biochemical data led to the assumption that the 30-kD porinlike pea protein was not present in chloroplasts but is restricted to proplastids only. This indicates the general relevance of the OEP24 as a general solute channel for plastid metabolism. The low substrate selectivity in vitro makes it probable that OEP24 functions as a general diffusion pore similar to porins in the outer envelope of Gram-negative bacteria and mitochondria. In line with this proposal, the open probability of the OEP24 channel is highest at 0 mV, which is similar to classic porins. Current evidence predicts that no significant membrane potential exists across the chloroplastic outer envelope (Douce and Joyard, 1990), resulting in an open OEP24 channel. Any other regulation mechanisms for OEP24 as they are predicted for porins remain to be established (Liu et al., 1994; Lee et al., 1996).

OEP24 conducts most tested solutes, including amino acids, that are also selectively channeled by OEP16. The existence of selective channels might be necessary and useful under limiting rates of metabolic substrates. In this case, the concentration of amino acids drops below a certain threshold value, requiring high-affinity channeling. In the outer membrane of Gram-negative bacteria, general diffusion pores and selective channels are also present side by side (reviewed in Nikaido, 1994). The electrophysiological characterization of purified outer envelope membranes indicates

the presence of additional channel-forming activity (Hinnah et al., 1997). Similar conclusions have been drawn from electrophysiological measurements by using either giant chloroplasts from Nitellopsis (Pottosin, 1992, 1993) or a mixed outer and inner envelope preparation from spinach (Heiber et al., 1995). However, in these studies, it was not possible to differentiate between voltage-gated channels of the outer and inner envelope membranes, respectively. Because the previously identified chloroplastic outer membrane channels Toc75 and OEP16 are involved in protein translocation and specific channeling of amino acids, respectively, OEP24 represents the only nonselective channel protein identified in the outer envelope of chloroplasts.

## METHODS

### cDNA Cloning and Overexpression

Sequence information was obtained by protease endoproteinase Glu-C (Boehringer Mannheim) digestion of SDS-PAGE purified OEP24 from chloroplastic outer envelope membranes (Cleveland, 1983). The deduced nucleotide sequences of the two peptides were used for a database search in dBEST. A homologous expressed sequence tag from rice (cDNA clone S3369; EMBL accession number D41099) was identified and used as a template to synthesize a random-primed digoxigenin-labeled probe by polymerase chain reaction (PCR), according to the manufacturer's recommendations (Boehringer Mannheim). A pea cDNA expression library (UniZAP XR; Stratagene, La Jolla, CA) was screened with this probe, resulting in the isolation of peacOEP24. Both strands were sequenced (Sanger et al., 1977). The cDNA sequence reported in this study has EMBL accession number AJ001009. A NdeI site was introduced at the first methionine of the coding region of peacOEP24 by PCR, using the forward primer 5′-GGGGGGCATATGAAGGCCGCTTTGAAGGGC-AAATACGAC-3′ and the universal primer. The PCR product was digested with NdeI and XhoI and ligated into pET21b, resulting in peacOEP24pet. Overexpression was done after transforming *Escherichia coli* BL21(DE3) cells (Novagen, Madison, WI). Recombinant OEP24 was recovered from insoluble inclusion bodies (Waegemann and Soll, 1995).

### Purification of Recombinant Protein

For further purification, the protein was dissolved in 6 M urea, 50 mM Hepes-KOH, pH 7.6, 1 mM EDTA, and 10 mM β-mercaptoethanol and passed over an anion exchange resin (Source Q; Pharmacia) as a first step of the purification protocol. OEP24 was recovered in the flowthrough and passed over a MonoS cation exchanger (Pharmacia) from which it was eluted at ~100 mM NaCl. The protein was dialyzed against water, freeze dried, and used for reconstitution experiments.

### Isolation of Membrane Vesicles

Pea (*Pisum sativum* var Golf) plants were grown for 12 to 14 days in a growth chamber under a 14-hr-light and 10-hr-dark regime. Intact chloroplasts were isolated from leaves and further purified by silica–sol gradients (Waegemann and Soll, 1991). After shrinking the intact chloroplasts (0.65 M sucrose and 20 mM Tricine, pH 7.9) and rupturing them with 50 strokes by using a Dounce homogenizer, thylakoids were spun down at 4000*g.* The supernatant was subjected to a further centrifugation at 200,000*g*, resulting in a membrane pellet that was used for separation of outer and inner membrane vesicles by sucrose density gradient centrifugation, according to Keegstra and Youssif (1986). The supernatant contained all soluble proteins and was described as the stromal extract. The thylakoids were washed at least twice (50 mM Na-Pi buffer, pH 7.4, and 10 mM NaCl) before further use. Mitochondrial membranes were isolated from potato mitochondria, according to Braun et al. (1992).

### Liposomes

Small liposomes were obtained by dissolving 50 mg/mL azolectin (type IV S; Sigma) in 10 mM Mops-Tris, pH 7.0, by using the microtip of a sonifier (Branson, Danbury, CT). Liposomes were freeze thawed once.

Insoluble inclusion bodies containing OEP24 were solubilized in 8 M urea, 80 mM MEGA-9 (Calbiochem, Bad Soden, Germany), and 10 mM Mops-Tris, pH 7.0, and mixed with the preformed liposomes to a final concentration of 0.1 mg of protein per 10 mg of azolectin. The suspension was freeze thawed and sonified in a supersonic bath. After 1.5 hr of incubation at room temperature, the suspension was dialyzed overnight against buffer containing 10 mM Mops-Tris, pH 7.0, at 4°C and used for bilayer measurements.

Purified OEP24 was resuspended in 80 mM MEGA-9, 6 M urea, and 10 mM Mops-Tris, pH 7.0, and reconstituted as described above.

### Circular Dichroism Spectroscopy

Circular dichroism (CD) spectra were measured by using a Jasco-J-720 spectropolarimeter (Jasco Labor- und Datentechnik GmbH, Gross-Umstadt, Germany) after calibration with (±)-10-camphorsulfonic acid. The spectra were recorded at 20°C in a quartz cell with a 0.5-cm optical length path. Scans were performed at a rate of 0.2 nm/sec and averaged ($n = 100$) to improve the signal/noise ratio. Both samples (OEP24 in 6 M urea and OEP24 liposomes) were adjusted to the same protein concentration: 50 ± 20 μg protein.

### Electrophysiological Measurements

Planar lipid bilayers were produced by using the painting technique (Mueller et al., 1962; Miller and White, 1984). A solution (1 μL) of 50 mg/mL L-α-azolectin in *n*-decan was applied to a hole (100 to 200 μm in diameter) in a Teflon septum, separating the two bath chambers (total volume ~3 mL each), which were equipped with magnetic stirrers. The resulting bilayers had a typical capacitance of ~0.5 μF/cm$^2$ and a resistance of >100 GΩ. The noise was ~1 pA (root mean square) at 5 kHz bandwidth. After a stable bilayer was formed in symmetrical solutions of 20 mM KCl and 10 mM Mops-Tris, pH 7.0, the solution of the *cis*-chamber was changed to asymmetrical concentrations (*cis*-chamber; 250 mM KCl, 10 mM $CaCl_2$, and 10 mM Mops-Tris, pH 7.0) by adding concentrated solutions of KCl and $CaCl_2$. The liposomes were added to the *cis*-compartment directly below the bilayer through the tip of a micropipette to allow the flow of

the liposomes across the bilayer. If necessary, the solution in the *cis*-chamber was stirred to promote fusion. After fusion, the electrolytes were changed to the final composition by perfusion. The Ag/AgCl electrodes were connected to the chambers through 2 M KCl–agar bridges. The electrode of the *trans*-compartment was connected directly to the headstage of a current amplifier (EPC 7; List-electronic, Darmstadt, Germany). Reported membrane potentials are referred to the *trans*-compartment. The amplified currents were recorded on a modified digital audio tape recorder digitized at a sampling interval of 0.2 msec and fed into an Axolab 1100 A/D converter (Axon Instruments, Foster City, CA) to store on the hard disk of an IBM-compatible personal computer. For analysis, a Windows-based analysis software (SCIP single channel investigation program) developed in our laboratory was used in combination with Origin 4.1 (Microcal Software Inc., Northampton, MA).

### Electrophysiologically Monitored Flux of Charged Solutes

The permeability ratio of the cation-to-anion fluxes of the charged solute was determined by measuring the equilibrium potential and by using the Nernst equation. Therefore, a 10-fold concentration gradient of the solute was used for all experiments.

### Electrophysiologically Monitored Osmotic Permeation Assay

Bilayers were produced as described above. A highly concentrated solution of the solute to be tested was then added to the *cis*-chamber to reach a final concentration of 250 mM. Concentrated $CaCl_2$ and KCl solutions were also added to a final concentration of 20 mM each (calcium was added only on the *cis*-side). Liposomes containing reconstituted OEP24 were applied as described above. A membrane potential of 100 mV was applied (*trans*-chamber positive). The pH of the solute stock solution was adjusted by using tetraethylamine (TEA)/OH and Hepes. Neither ion was able to promote fusion on its own. All other conditions were as outlined previously (Miller et al., 1976; Woodbury and Miller, 1990).

### Optical Measurements

Time scan (duration, 2 min) absorbance measurements were performed in an Aminco DM2000 UV-Vis spectrophotometer (SLM-Aminco; Spectronic Instruments, Inc., Rochester, NY) at 400 nm. Liposomes equivalent to an optical density of 0.15 to 0.2 were equilibrated in 1 mL of a solution containing 10 mM TEA-Hepes, pH 7, and 10 mM KCl. The absorbance at 400 nm was monitored for 15 sec, and the osmotically active solute was added from a 1 M stock solution (in the case of ATP, a 200 mM stock was used). After stirring for 10 sec, the change of absorbance was monitored continuously up to 2 min. The pH of the stock solutions was titrated by addition of TEA/OH or solid Hepes, when required. The relative changes of the turbidity at 400 nm were calculated according to

$$(\Delta A/A) = \frac{A_{\text{baseline}} - A_{\text{sat}}}{A_{\text{baseline}}},$$

where $A_{\text{baseline}}$ is the average absorbance ($i = 10$ sec) before the addition of the osmoticum, and $A_{\text{sat}}$ is the average absorbance during the last 10 sec of the measuring interval of 120 sec. When required, the apparent absorbance changes were corrected for those resulting from changes in the refractive index after addition of the osmoticum.

## ACKNOWLEDGMENTS

This work was supported by the Deutsche Forschungsgemeinschaft and Fonds der Chemischen Industrie.

Received February 19, 1998; accepted May 11, 1998.

## REFERENCES

**Allen, G.J., and Sanders, D.** (1995). Calcineurin, a type 2B protein phosphatase, modulates the $Ca^{2+}$-permeable slow vacuolar ion channel of stomatal guard cells. Plant Cell **7,** 1473–1483.

**Anderson, J.W.** (1990). Sulfur metabolism in plants. In The Biochemistry of Plants, Vol. 16, B.J. Miflin and P.J. Lea, eds (New York: Academic Press), pp. 328–375.

**Benz, R.** (1994). Permeation of hydrophilic solutes through mitochondrial outer membranes: Review on mitochondrial porins. Biochim. Biophys. Acta **1197,** 167–196.

**Braun, H.P., Emmermann, M., Kruft, V., and Schmitz, U.K.** (1992). Cytochrome c1 from potato: A protein with a presequence for targeting to the mitochondrial intermembrane space. Mol. Gen. Genet. **231,** 217–225.

**Claros, M.G., and von Heijne, G.** (1994). TopPredII: An improved software for membrane protein structure predictions. Cabios **10,** 685–686.

**Cleveland, P.W.** (1983). Peptide mapping in one dimension by limited proteolysis of sodium dodecylsulfate solubilized proteins. Methods Enzymol. **96,** 222–229.

**Cowan, S.W., Schirmer, T., Rummel, G., Steinert, M., Ghosh, R., Paupit, R.A., Jansonius, J.N., and Rosenbusch, J.P.** (1992). Crystal structures explain functional properties of two *E. coli* porins. Nature **358,** 727–733.

**Crawford, N.M.** (1995). Nitrate: Nutrient and signal for plant growth. Plant Cell **7,** 859–868.

**DeLa Vega, A., and Delcour, A.H.** (1996). Polyamines decrease *Escherichia coli* outer membrane permeability. J. Bacteriol. **178,** 3715–3721.

**De Pinto, V., Prezioso, G., Thinnes, F.P., Link, T.A., and Palmieri, F.** (1991). Peptide-specific antibodies and proteases as probes of the transmembrane topology of the heart mitochondrial porin. Biochemistry **30,** 10191–10206.

**Douce, R., and Joyard, J.** (1990). Biochemistry and function of the plastid envelope. Annu. Rev. Cell Biol. **6,** 173–216.

**Fischer, K., Weber, A., Brink, S., Arbinger, B., Schünemann, D., Borchert, S., Heldt, W., Popp, B., Benz, R., Link, T.A., Eckerskorn, C., and Flügge, U.-I.** (1994). Porins from plants. J. Biol. Chem. **269,** 25754–25760.

**Fischer, K., Kammerer, B., Gutensohn, M., Arbinger, B., Weber, A., Häusler, R.E., and Flügge, U.-I.** (1997). A new class of plastidic phosphate translocators: A putative link between primary and secondary metabolism by the phosphoenolpyruvate/phosphate antiporter. Plant Cell **9,** 453–462.

**Flügge, U.-I., and Benz, R.** (1984). Pore-forming activity in the outer membrane of the chloroplast envelope. FEBS Lett. **169,** 85–89.

**Flügge, U.-I., and Heldt, H.W.** (1991). Metabolite translocators of the chloroplast envelope. Annu. Rev. Plant Physiol. Plant Mol. Biol. **42,** 129–144.

**Fujiki, Y., Hubbard, A.L., Fowler, S., and Lazarow, P.B.** (1982). Isolation of intracellular membranes by means of sodium carbonate treatment: Application to endoplasmic reticulum. J. Cell Biol. **93,** 97–102.

**Heiber, T., Steinkamp, T., Hinnah, S., Schwarz, M., Flügge, U.-I., Weber, A., and Wagner, R.** (1995). Ion channels in the chloroplast envelope membrane. Biochemistry **34,** 15906–15917.

**Heins, L., Mentzel, H., Schmid, A., Benz, R., and Schmitz, U.K.** (1994). Biochemical, molecular and functional characterization of porin isoforms from potato mitochondria. J. Biol. Chem. **269,** 26402–26410.

**Heins, L., Collinson, I., and Soll, J.** (1998). The protein translocation apparatus of chloroplast envelopes. Trends Plant Sci. **3,** 56–61.

**Hille, B.** (1992). Ionic Channels of Excitable Membranes. (Sunderland, MA: Sinauer Associates).

**Hinnah, S., Hill, K., Wagner, R., Schlicher, T., and Soll, J.** (1997). Reconstitution of a chloroplast protein import channel. EMBO J. **6,** 7351–7360.

**Keegstra, K., and Youssif, A.E.** (1986). Isolation and characterization of chloroplast envelope membranes. Methods Enzymol. **118,** 316–325.

**Kyte, J., and Doolittle, R.F.** (1982). A simple method for displaying the hydrophobic character of a protein. J. Mol. Biol. **157,** 105–132.

**Lee, A.-C., Xu, X., and Colombini, M.** (1996). The role of pyridine dinucleotides in regulating the permeability of the mitochondrial outer membrane. J. Biol. Chem. **271,** 26724–26731.

**Liu, M.Y., Torgrimson, A., and Colombini, M.** (1994). Characterization and partial purification of the VDAC-channel-modulating protein from calf liver mitochondria. Biochim. Biophys. Acta **1185,** 203–212.

**Lübeck, J., Heins, L., and Soll, J.** (1997). Protein import into chloroplasts. Physiol. Plant. **100,** 53–64.

**Miller, C., and White, M.M.** (1984). Dimeric structure of single chloride channels from Torpedo electroplax. Proc. Natl. Acad. Sci. USA **81,** 2772–2775.

**Miller, C., Arvan, P., Telford, J.N., and Racker, E.** (1976). $Ca^{2+}$ induced fusion of proteoliposomes: Dependence on transmembrane osmotic gradient. Cell **9,** 271–282.

**Mueller, P., Rudin, D.O., Tien, H., and Westcott, W.C.** (1962). Reconstitution of cell membrane structure in vitro and its transformation into an excitable system. Nature **194,** 979–980.

**Neuhaus, H.E., Thom, E., Möhlmann, T., Steup, M., and Kampfenkel, K.** (1997). Characterization of a novel eukaryotic ATP/ADP translocator located in the plastid envelope of *Arabidopsis thaliana* L. Plant J. **11,** 73–82.

**Nikaido, H.** (1994). Porins and specific diffusion channels in bacterial outer membranes. J. Biol. Chem. **269,** 3905–3908.

**Pohlmeyer, K., Soll, J., Steinkamp, T., Hinnah, S., and Wagner, R.** (1997). Isolation and characterization of an amino acid–selective channel protein present in the chloroplastic outer envelope membrane. Proc. Natl. Acad. Sci. USA **94,** 9504–9509.

**Pottosin, I.I.** (1992). Single channel recordings in the chloroplast envelope. FEBS Lett. **308,** 87–90.

**Pottosin, I.I.** (1993). One of the chloroplast envelope ion channels is probably related to the mitochondrial VDAC. FEBS Lett. **330,** 211–214.

**Preiss, M., Rosidi, B., Hoppe, P., and Schulz, G.** (1993). Competition of $CO_2$ and acetate as substrates for fatty acid synthesis in immature chloroplasts of barley seedlings. J. Plant Physiol. **142,** 525–530.

**Sanger, F., Nicklen, S., and Coulsen, A.R.** (1977). DNA sequencing with a chain terminating inhibitor. Proc. Natl. Acad. Sci. USA **74,** 5463–5467.

**Sreerama, N., and Woody, R.W.** (1994). Protein secondary structure from circular dichroism spectroscopy. Combining variable selection principle and cluster analysis with neutral network, ridge regression and self-consistent methods. J. Mol. Biol. **242,** 497–507.

**Viera, L.I., Senistra, G.A., and Disalvo, E.A.** (1996). Changes in the optical properties of liposome dispersions in relation to the interlamellar distance and solute interaction. Chem. Physics Lipids **81,** 45–54.

**Waegemann, K., and Soll, J.** (1991). Characterization of the protein import apparatus in isolated outer envelopes of chloroplast. Plant J. **1,** 149–159.

**Waegemann, K., and Soll, J.** (1995). Characterization and isolation of the chloroplast protein import machinery. In Methods in Cell Biology, D.W. Galbraith, D.W. Bourque, and H.J. Bohnert, eds (San Diego, CA: Academic Press), pp. 255–267.

**Weber, A., Menzlaff, E., Arbinger, B., Gutensohn, M., Eckerskorn, C., and Flügge, U.-I.** (1995). The 2-oxoglutarate/malate translocator of chloroplast envelope membranes: Molecular cloning of a transporter containing a 12-helix motif and expression of the functional protein in yeast cells. Biochemistry **34,** 2621–2627.

**Woodbury, J., and Miller, C.** (1990). Nystatin-induced liposome fusion. Biophys. J. **68,** 833–839.

**Yoshikawa, W., Akutsu, H., and Kyogoku, Y.** (1983). Light-scattering properties of osmotically active liposomes. Biochim. Biophys. Acta **735,** 397–406.